INTERNATIONAL JOURNAL OF CIRCUIT THEORY AND APPLICATIONS
Int. J. Circ. Theor. Appl. (2010)
Published online in Wiley InterScience (www.interscience.wiley.com). DOI: XX.XXXX/cta.XXX

Improved static and dynamic performances of a two-cell DC-DC buck converter using a digital dynamic time delayed control

K. Kaoubaâ[1], J. Pelaez-Restrepo[2], M. Feki[1], B. G. M. Robert[3], and A. El Aroudi[2,*]

[1]*Research unit ICOS, École Nationale d'Ingénieurs de Sfax, Sfax, Tunisia*
[2]*GAEI Research Group, Departament d'Enginyeria Electrònica, Elèctrica i Automàtica (DEEEA) Universitat Rovira i Virgili, Tarragona, Spain*
[3]*Laboratoire CReSTIC, Université de Reims-Champagne-Ardenne,Reims, France*

SUMMARY

Multi-cell converters have been developed to overcome shortcomings in usual switching devices. The control system in these circuits is twofold: first, to balance voltages of the switches and second to regulate the load current to a desired value. However, with a purely proportional controller, the system presents a static error. With a PI controller the static error is annihilated, but at the expense of shortening the stability region and increasing settling time. In this work, a zero static error dynamic controller for a two-cell DC-DC buck converter is designed. To achieve zero current error, we propose a generalized scheme of a dynamic controller. Then, using nonlinear analysis and Lyapunov stability theory and bifurcation prediction tools, we prove that zero static error is achieved. The proposed controller outperforms the PI controller in terms of settling time in the presence of saturating effect during the start-up transients. Numerical simulations in the form of time domain waveforms and bifurcation diagrams from switched circuit-based model are presented to confirm our theoretical results.

KEY WORDS: Multi-cell converter; Digital control; Lyapunov stability, Subharmonics, Dynamic TDFC

*Correspondence to: Abdelali El Aroudi, Departament d'Enginyeria Electrònica, Elèctrica i Automàtica (DEEEA), Universitat Rovira i Virgili, Tarragona, Spain.
†E-mail: abdelali.elaroudi@urv.cat

Received XX YY ZZZZ
Revised XX YY ZZZZ

1. Introduction

Multi-cell converters have been developed to overcome shortcomings in solid-state switching device ratings so that to reduce their stress [1]. Because distributed power sources, such as PV panels, wind turbine and fuel cells, are becoming increasingly prevalent, the use of such converters to control the current and voltage output directly from renewable energy sources will provide significant advantages because of their fast response and autonomous control [2], [3]. Multi-cell converters applications include speed variation for medium and high voltage motors, voltage dynamic restoration and harmonics filtering [4]. Readers interested in application of multi-cell converter may see [5]. Recently, they have been also proposed for efficient wide-bandwidth envelope tracking in radio frequency power amplifiers [6]. An appropriate functioning of these systems requires a control circuit with the main aim to achieve good performances in front of external perturbations, parametric uncertainty and load demands. With an appropriate control strategy, it was demonstrated that multi-cell power electronic converters can have exceptional performances in transients and in steady state. The goal of the control is to balance the flying capacitor voltage to a fraction of the input voltage and to adjust the load current to an appropriate reference level [1]. This is achieved by controlling the ON/OFF time durations of the switches.

In most modern power electronics converters, there is a need to control the averaged value of one or more of the system variables with a fixed switching frequency [7]. Furthermore, controllers are required to ensure satisfactory transient and steady-state behavior for these systems. Traditionally, control action is usually based on an error signal defined as the difference between the reference and the actual values of the state to be controlled. These controllers that manipulates the error signal to determine the desired control action has classically been an analog system. Many control approaches can be used for modern power converters [8]-[11]. In [8], the authors use a sliding mode approach to design a controller for a two-cell converter. The main drawback of this control technique, despite its popularity, is a variable switching frequency and undesired chattering effects. In [9], a global hybrid dynamical approach is used while a backstepping solution with current mode control have been studied in [10]. One cycle control have been studied for power converters working in both continuous and discontinuous conduction modes in [11].

In the last few decades, analog controllers have often been substituted by digital controllers, whose inputs and outputs are defined at discrete time, in many applications. Digital control offers many advantages over analog control that explain its wide popularity in recent literature. Some of these advantages are: accuracy, negligible implementation error and flexibility. Also, the speed of computer hardware has increased exponentially since the 1980s. This increase in processing speed has made it possible to sample and process control signals at very high

frequencies. Another advantage is that the cost of digital circuitry continues to decrease. Nevertheless, it has been shown that power converters in general and multi-cell DC-DC converters in particular may exhibit subharmonic oscillation and chaotic behavior under traditional controllers [12]-[17]. As a matter of fact, the chaotic behavior usually emerges from bad tuning of the system parameters [18]-[20]. An advantage of digital controllers is that the corresponding discrete time model can be obtained in closed form ([16], [20]) and many of the undesired phenomena can be predicted, analyzed and even avoided by using sophisticated controllers [21]. For instance time delayed feedback control (TDFC) and its extended version (ETDFC) were used to stabilize the unstable periodic orbits embedded in the chaotic attractor [22]. There the TDFC technique has been applied to a single cell buck converter and its stability domain were obtained combining analytical methods based on Floquet theory and numerical root finding algorithms. However, the implementation of the proposed control can not be carried out in practice. Also, despite a wider stability region for these controllers, the static error could not be annihilated. Of course, a digital PI controller can be used to annihilate the static error but it will be shown later that due to saturation effect during transient, the system response is very slow and the over-shoot are high even with an optimized design based on linear techniques. Moreover, an exact analog implementation of time delayed feedback is not possible because of the need of an infinite memory. A TDFC has an obvious advantage of a simple experimental implementation if the delay is digitalized. However, it is well known that a system with an odd number of eigenvalues outside the unit circle can not be stabilized by a static TDFC due to the so called *odd number limitation* [23]. A dynamic TDFC can be used in this case [24] where, a necessary and sufficient condition for stabilization have been derived and a design method of reduced order chaos controller has been shown by using linear matrix inequalities (LMIs). The main drawback of the approach in [24] that the LMIs have to be solved numerically.

In this paper, a solution based on a dynamic digital TDFC algorithm is proposed for stabilizing the dynamics of a two-cell DC-DC buck converter. A zero static error dynamic control technique with a wide stability margin will be developed and analyzed for this system. It will be shown that the proposed technique is a powerful strategy for avoiding subharmonic oscillations and chaotic behavior while eliminating the static error even in the presence of duty cycle saturation outperforming the traditional PI controller in terms of settling time. The general model can be expressed as a cascaded system and by applying Lyapunov theory we obtain the stability domain.

The rest of the paper is organized as follows: in Sec. 2, the system discrete-time model is presented. In Sec. 3, the generalized dynamic controller is synthesized. In Sec. 4, the stability of the system under the synthesized controller is studied analytically. Some numerical simulations from the derived model are shown in the same section confirming the theoretical predictions.

Circuit-based simulations are presented in Sec. 5 to validate the controller performances obtained from the derived model and theoretical analysis. Finally, in the last section, some concluding remarks of this work are summarized.

2. Modeling the Two-Cell Converter

2.1. System description

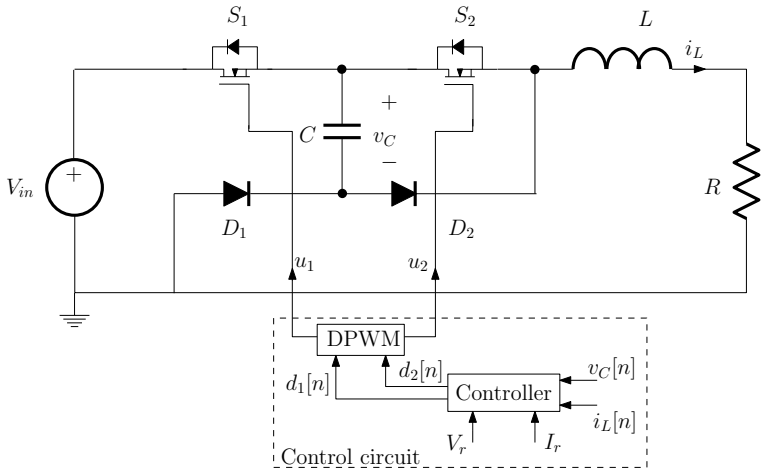

Figure 1. A basic two-cell DC-DC buck converter.

The converter that we will deal with in this paper is depicted in Fig.1. It is based on a buck chopper modified in order to allow a higher input voltage by using two serial switches (transistors or diodes). The role of the controller is twofold: first, to balance the switch voltages and therefore to achieve a constant average voltage v_C equal to one half the input voltage V_{in} and second, to regulate the inductor output current i_L to a desired value I_r according to the demands of the load. It is worth noting here that if the floating capacitor voltage v_C is equal to one half the input voltage, the total stress is shared equally between both switches making this structure suitable for high voltage applications [4]. The binary command signals u_1 and u_2 are the outputs of a digital pulse width modulator (DPWM) driven by the controller which will be designed to define the variables d_1 and d_2 of the binary signals u_1 and u_2. These variables are defined in this paper as the fraction of the switching period T during which the switch S_k is open (OFF state) and being then complementary to the actual duty cycles. Thus, the switch S_k will remain in its OFF state during d_kT when it is driven by a control signal u_k with a duty cycle d_k. We assume here that the binary control signals u_1 and u_2 are phase shifted by π

in order to obtain optimum waveforms for the inductor current. That is, the inductor current frequency is twice the switching frequency in this case [1]. In a typical operating mode the switch S_k and the diode D_k are turned ON and OFF in a cyclic and complementary manner under the action of a DPWM. When the switch S_k is closed the diode D_k is open and vice versa. Centered pulses, during a switching period, will be used for the switches in such a way that the reference signals will correspond to the averaged variables in steady state operation [20].

2.2. Switched model

By applying Kirchhoff laws to the two-cell converter, the following switched model is obtained:

$$\frac{d}{dt}\begin{pmatrix} i_L \\ v_C \end{pmatrix} = \begin{pmatrix} -\frac{R}{L} & (u_2-u_1)\frac{1}{L} \\ (u_1-u_2)\frac{1}{C} & 0 \end{pmatrix}\begin{pmatrix} i_L \\ v_C \end{pmatrix} + \begin{pmatrix} \frac{V_{in}}{L}u_1 \\ 0 \end{pmatrix} \tag{1}$$

where u_k are the binary command signals for the switches S_k given by:

$$u_k = \begin{cases} 1 & \text{if} \quad S_k \quad \text{is closed (ON)} \\ 0 & \text{if} \quad S_k \quad \text{is open (OFF)} \end{cases} \tag{2}$$

Clearly, when u_1 and u_2 are replaced by their values 1 or 0, we obtain a linear system for each topology. Consequently, we can obtain closed form solution for each different topology. This fact is crucial for obtaining the discrete-time model of the two-cell converter.

2.3. Discrete time model

By stacking-up the closed form solutions and assuming rectilinear waveforms for the state variables, the nonlinear discrete time mode can be obtained. However, in order to be able to perform mathematical analysis, this discrete time mode will be simplified by using some practical assumptions. Namely, the time constants RC and L/R of the circuit are assumed to be much smaller than the switching period T. Therefore, the following approximated model is obtained:

$$\begin{pmatrix} i_L[n+1] \\ v_C[n+1] \end{pmatrix} = \begin{pmatrix} 1-\frac{TR}{L} & (d_1[n]-d_2[n])\frac{T}{L} \\ (d_2[n]-d_1[n])\frac{T}{C} & 1 \end{pmatrix}\begin{pmatrix} i_L[n] \\ v_C[n] \end{pmatrix} + \begin{pmatrix} \frac{V_{in}T}{L}(1-d_1[n]) \\ 0 \end{pmatrix} \tag{3}$$

For the sake of reducing the number of parameters of the system we will consider some new dimensionless variables, where the current is scaled by the maximum current available in the circuit ($I_{max} = \frac{V_{in}}{R}$), the voltage is scaled by the maximum voltage V_{in} and time is normalized by the switching period T. Let us therefore consider the following changes of variables and parameters:

Variables:

$$x_i[n] = \frac{Ri_L[n]}{V_{in}}, \;\; x_v[n] = \frac{v_C[n]}{V_{in}} \quad \text{and}$$

Parameters:

$$\delta_L = \frac{RT}{L},\ \ \delta_C = \frac{T}{RC}$$

Therefore, we obtain the following dimensionless model:

$$\begin{pmatrix} x_i[n+1] \\ x_v[n+1] \end{pmatrix} = \begin{pmatrix} 1-\delta_L & (d_1[n]-d_2[n])\delta_L \\ (d_2[n]-d_1[n])\delta_C & 1 \end{pmatrix} \begin{pmatrix} x_i[n] \\ x_v[n] \end{pmatrix} + \begin{pmatrix} \delta_L(1-d_1[n]) \\ 0 \end{pmatrix} \tag{4}$$

In order to reduce the current ripple through the load and the voltage ripple across the capacitor, the circuit parameters should satisfy $\delta_L \ll 1$ and $\delta_C \ll 1$. These assumptions also make the hypothesis of rectilinear waveform solutions tenable. The above model will be used for theoretical analysis and design, all along caring to check the performances of the suggested control method on the circuit-based switching model. In the sequel, simulations will be carried out with the following parameters:

$$\delta_L = 0.1,\quad \delta_C = 0.1,\quad I_r = 0.6 \ \text{ and } \ V_r = 0.5 \tag{5}$$

3. Digital dynamic controller design

3.1. Transfer functions in the z domain

Usually, the controller of a power electronics dc-dc converter is designed based on a small-signal model of the system [7]. By linearizing the bilinear discrete time model and taking the z transform, the control-to-output transfer function matrix for the open loop system can be obtained. Let us consider that the the vector of the state variables x can be expressed as the sum of the steady state value x^* and a small disturbance $\hat{x}$ ($x_i = x_i^* + \hat{x}_i$ and $x_v = x_v^* + \hat{x}_v$). By substituting these expressions in (4)

$$\begin{aligned} x_i^* + \hat{x}_{i,n+1} &= (1-\delta_L)(x_i^* + \hat{x}_{i,n+1}) + [(d_1^* + \hat{d}_{1,n}) - (d_2^* + \hat{d}_{2,n})]\delta_L(x_v^* + \hat{x}_v) \\ &\quad +\delta_L(1 - (d_1^* + \hat{d}_{1,n})) \\ x_v^* + \hat{x}_{v,n+1} &= [(d_2^* + \hat{d}_{2,n}) - (d_1^* + \hat{d}_{1,n})]\delta_C(x_i^* + \hat{x}_i) + x_v^* + \hat{x}_{v,n+1} \end{aligned} \tag{6}$$

By performing a linearization in the vicinity of the equilibrium point $x^* = (x_i^*, x_v^*)^t$, the following open loop small signal z domain model is obtained for the system

$$\hat{\mathbf{x}}(z) = \mathbb{H}(z)\hat{\mathbf{d}}(z) \tag{7}$$

where $\hat{\mathbf{x}}(z)$ stands for the z transform of the small signal state vector $\hat{x}$, $\hat{\mathbf{d}}(z)$ is the z transform of the small signal vector of duty cycles d_1 and d_2 and $\mathbb{H}$ is the matrix transfer function given by:

$$\mathbb{H} = \begin{pmatrix} H_{11}(z) & H_{12}(z) \\ H_{21}(z) & H_{22}(z) \end{pmatrix} \tag{8}$$

where

$$\begin{aligned} H_{11}(z) &= \frac{\hat{x}_i}{\hat{d}_1} = \frac{\delta_L(1-x_v^*)}{z-(1-\delta_L)} \\ H_{12}(z) &= \frac{\hat{x}_v}{\hat{d}_1} = \frac{x_i^*}{z-1} \\ H_{21}(z) &= \frac{\hat{x}_i}{\hat{d}_2} = -\frac{\delta_L x_v^*}{z-(1-\delta_L)} \\ H_{22}(z) &= \frac{\hat{x}_v}{\hat{d}_2} = -\frac{x_i^*}{z-1} \end{aligned} \tag{9}$$

x_i^* is the steady state value of the dimensionless current x_i. It can be observed that the open loop transfer function corresponding to the voltage loop is a pure accumulator while that corresponding to the current loop is a low-pass filter. Therefore, a zero static error can be achieved without inserting an extra state variable in the voltage loop. However, in order to get a zero static error for the load current, a dynamic controller must be used for this loop. Therefore, in addition to the proportional terms, an extra dynamic term will be added to the expression of the duty cycles which constitutes the input the system studied. The control law is then as follows:

$$d_1[n] = k_i(x_i[n]-I_r) + k_v(x_v[n]-V_r) + d_\ell[n] \tag{10}$$

$$d_2[n] = k_i(x_i[n]-I_r) - k_v(x_v[n]-V_r) + d_\ell[n] \tag{11}$$

where $d_\ell[n]$ is the output of a dynamical system that we choose it to be a first order and linear in this context and depending only on the load current in order not to add analysis difficulty:

$$x_d[n+1] = \alpha x_d[n] + \beta\epsilon[n] \tag{12}$$

$$d_\ell[n] = \gamma x_d[n] + \delta\epsilon[n] \tag{13}$$

where $\epsilon[n]$ is the input of the dynamic controller which is a feedback current error that depends on the system state. α, β, γ and δ are the controller scalar constant parameters to be designed. As mentioned above, centered pulses, during a switching period, are used for the switches in such a way that the reference signals correspond to the averaged variables in steady state operation [20].

We implicitly understand from any expression of the duty cycles d_1 and d_2 that they may undergo a saturation because they neither can be negative, nor greater than one because the OFF state can not be larger than the switching period. Therefore, the applied duty cycle is in fact $\mathrm{sat}(d_k)$ and not d_k, where $\mathrm{sat}(d)$ is the function defined by:

$$\mathrm{sat}(d) = \frac{1}{2}\left(1+|d|-|d-1|\right) \tag{14}$$

One way to annihilate the static error is to use the discrete time PI controller which can be represented by the following recurrent form:

$$d_\ell[n] = \frac{k_i}{\tau_i}\sum_{k=0}^{n}\epsilon[k] = d_\ell[n-1] + \frac{k_i}{\tau_i}\epsilon[n] \tag{15}$$

where τ_i is the integral time constant and $\epsilon[n] = x_i[n] - I_r$ is the error between the current state and its reference value. Hence, using the representation (12)-(13), the dynamical representation of the integral controller is

$$x_d[n+1] = x_d[n] + \frac{k_i}{\tau_i}\epsilon[n] \tag{16}$$

$$d_\ell[n] = x_d[n] + \frac{k_i}{\tau_i}\epsilon[n] \tag{17}$$

where, if compared to (12), the controller parameters are $\alpha = \gamma = 1$ and $\beta = \delta = \frac{k_i}{\tau_i}$. It has been shown in [20] that the two-cell buck converter under the PI controller presents subharmonic oscillations and chaos when the current gain is increased with the purpose to increase the system response speed. In what follows, a dynamic time delayed controller is designed in discrete time with the aim to improve the settling time while widening the stability range with respect to k_i.

3.2. Generalized dynamic time-delayed feedback controller

In this section, we present a stability analysis of the dynamic controller with a time delayed feedback in its general form. Therefore, the duty cycles have a similar form as (10)-(11) but with $d_\ell[n]$ the output of the following dynamic system

$$x_d[n+1] = \alpha x_d[n] + \beta(x_i[n] - x_i[n-1]) \tag{18}$$

$$d_\ell[n] = \gamma x_d[n] + \delta(x_i[n] - x_i[n-1]) \tag{19}$$

By application of this controller, the closed loop system is a fourth order system due to the introduction of $x_d[n]$ and $x_i[n-1]$. Let us define the following new state variables:

$$x[n] = \begin{pmatrix} x_1[n] \\ x_2[n] \\ x_3[n] \\ x_4[n] \end{pmatrix} = \begin{pmatrix} x_v[n] \\ x_i[n-1] \\ x_i[n] \\ x_d[n] \end{pmatrix} \tag{20}$$

Therefore we obtain the closed loop system described by:

$$x_1[n+1] = x_1[n] - 2k_v\delta_C\big(x_1[n] - V_r\big)x_3[n] \tag{21}$$

$$x_2[n+1] = x_3[n] \tag{22}$$

$$x_3[n+1] = 2k_v\delta_L\Big(x_1[n] - V_r\Big)x_1[n] + \big(1-\delta_L\big)x_3[n] + \delta_L\Big(1 - k_i(x_3[n] - I_r) - k_v(x_1[n] - V_r) - \gamma x_4[n] - \delta(x_3[n] - x_2[n])\Big) \tag{23}$$

$$x_4[n+1] = \alpha x_4[n] + \beta(x_3[n] - x_2[n]) \tag{24}$$

Let's determine the fixed point of this system. Actually, according to the value of α we can distinguish two different cases:

case 1: $0 \leq \alpha < 1$ where $x_1^* = V_r$, $x_2^* = x_3^* = \frac{1+k_i I_r}{1+k_i}$ and $x_4^* = 0$.
case 2: $\alpha = 1$ where $x_1^* = V_r$, $x_2^* = x_3^*$ and $x_3^* = \frac{1+k_i I_r - \gamma x_4^*}{1+k_i}$

Clearly, in case 1, the reference current can not be achieved unless k_i is raised to infinity, thus making this case worthless. However, the second case is more interesting because there are infinitely many fixed points that define a line in the plane $x_4 - x_3$; and if x_4^* is stabilized at $\frac{1-I_r}{\gamma}$ then $x_3^* = I_r$ becomes a fixed point as required. To stabilize x_4^* at $\frac{1-I_r}{\gamma}$ we may need to modify the dynamic controller given by (18) as follows:

$$x_d[n+1] = x_d[n] - k_{x,d}\Big(x_d[n] - \frac{1-I_r}{\gamma}\Big) + \beta(x_i[n] - x_i[n-1]) \quad (25)$$

$$d_\ell[n] = \gamma x_d[n] + \delta(x_i[n] - x_i[n-1]) \quad (26)$$

with this choice, we clearly have the fixed point

$$x_1^* = V_r\ , \qquad x_2^* = x_3^* = I_r\ , \qquad \text{and} \qquad x_4^* = \frac{1-I_r}{\gamma}$$

Therefore, we just need to fixe the design parameters to achieve the stability of the fixed point.

4. Global stability of the system subject to the generalized dynamic controller

In [24] a necessary and sufficient condition for stability have been derived based on LMIs. The main drawback of the approach in [24] that the LMIs have to be solved numerically. In this work, it will be shown that the general model of the two-cell buck converter can be expressed as a cascaded system ([25]) and by applying Lyapunov theory we obtain the stability domain. Let us define the error state $e[n] = x[n] - x^*$ hence we get:

$$e_1[n+1] = e_1[n] - 2k_v\delta_C e_1[n]\big(e_3[n] + I_r\big) \quad (27)$$

$$e_2[n+1] = e_3[n] \quad (28)$$

$$e_3[n+1] = \big(1 - \delta_L(1+k_i+\delta)\big)e_3[n] + \delta_L\delta e_2[n] + k_{x,d}\delta_L e_1[n]\ldots \ldots(2e_1[n] + 2V_r - 1) - \delta_L\gamma e_4[n] \quad (29)$$

$$e_4[n+1] = (1-k_{x,d})e_4[n] + \beta(e_3[n] - e_2[n]) \quad (30)$$

By taking into account that $2V_r - 1 = 0$, then the error system may be written in the form

$$e[n+1] = \mathbb{A}e[n] + f(e[n]) \quad (31)$$

where

$$\mathbb{A} = \begin{pmatrix} 1-2k_v\delta_C I_r & 0 & 0 & 0 \\ 0 & 0 & 1 & 0 \\ 0 & \delta_L\delta & 1-\delta_L(1+k_i+\delta) & -\delta_L\gamma \\ 0 & -\beta & \beta & 1-k_{x,d} \end{pmatrix}, \qquad f = \begin{pmatrix} -2\overline{k_v}\delta_C e_1[n]e_3[n] \\ 0 \\ 2\overline{k_v}\delta_L e_1[n]^2 \\ 0 \end{pmatrix}$$

Of course $\overline{k_v} = k_v$; but we notice that f only depends on the design parameter $\overline{k_v}$; so if we may choose design parameters $k_v = k_v^s$, $k_i = k_i^s$, $\beta = \beta^s$, $\gamma = \gamma^s$, $\delta = \delta^s$ and $k_{x,d} = k_{x,d}^s$ such that $\mathbb{A}$ is stable, then there exists $\overline{k_{v\max}}$ such that if $\overline{k_v} < \overline{k_{v\max}}$ then

$$e[n+1] = \mathbb{A}e[n] + f(e[n]) \tag{32}$$

is locally asymptotically stable. Moreover, if we can show that $\overline{k_{v\max}} > k_v^s$, then the stability of the system is proved. Clearly, the stability of $\mathbb{A}$ depends on the position of its eigenvalues with respect to the unit circle. First, we easily verify that it has an eigenvalue at $\lambda = 1 - 2k_v\delta_C I_r$. To make this eigenvalue as fast as possible, one should place it at the origin by choosing $k_v = \frac{1}{2\delta_C I_r}$. In fact, this value makes k_v at a large amplitude, hence requiring $\overline{k_v}$ to go equally large. Therefore, we might be having a trade off in this regard. The rest of the eigenvalues are roots of the following characteristic equation:

$$z^3 + \big(\delta_L(1+k_i+\delta) + k_{x,d} - 2\big)z^2 + \Big((k_{x,d}-1)\big(\delta_L(1+k_i+\delta)-1\big) + \delta_L(\beta\gamma-\delta)\Big)z + \cdots$$
$$\cdots \delta_L(\delta(1-k_{x,d}) - \beta\gamma) = 0 \tag{33}$$

Should we look at equation (30), then intuitively, we may choose $k_{x,d} = 1$ to have a fast convergence of the dynamic controller state error e_4. With this choice, Jury's stability criterion requires the following:

$$1 > \mid \delta_L\beta\gamma \mid \tag{34}$$

$$1 - (\delta_L\beta\gamma)^2 > \delta_L\Big(\delta_L\beta\gamma(1+k_i+\delta) - \delta\Big) \tag{35}$$

$$\delta_L(1+k_i) > 0 \tag{36}$$

$$2(1+\delta_L\beta\gamma) > \delta_L(1+k_i+2\delta) \tag{37}$$

First, we note that parameters β and γ appear always in a product form and according to (34), we have

$$-\frac{1}{\delta_L} < \beta\gamma < \frac{1}{\delta_L} \tag{38}$$

which gives the shaded region shown in Fig. 2. Inequality (36) implies that $k_i > -1$ which is always satisfied since we always considered positive values of k_i. Inequalities (35) and (37) imply

$$\frac{\delta_L\beta\gamma}{1-\delta_L\beta\gamma}(1+k_i) - \frac{1+\delta_L\beta\gamma}{\delta_L} < \delta < -\frac{1}{2}(1+k_i) + \frac{1+\delta_L\beta\gamma}{\delta_L} \tag{39}$$

For different signs of the product $\beta\gamma$, Fig. 3-a delineates shaded areas corresponding to stability region in the parameter space $k_i - \delta$. Note that $\beta\gamma = 0$ when $\beta = 0$ because γ cannot be zero since it appears in the denominator of x_4^*. For negative values of $\beta\gamma$, the stability region extends to larger values of k_i. However, for positive values of $\beta\gamma$ the stability may only be obtained for

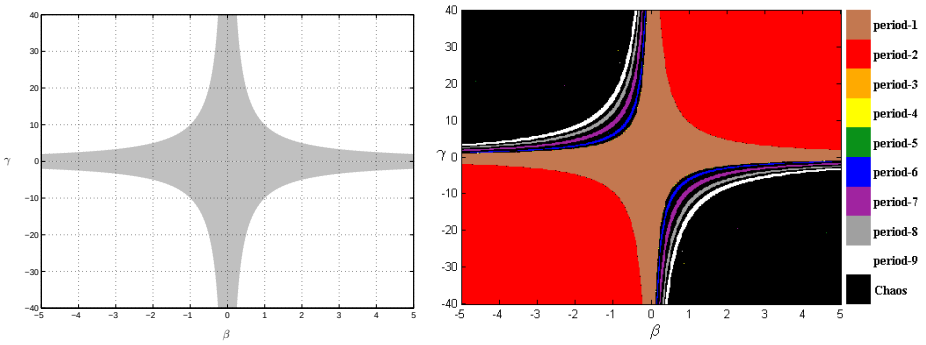

(a) (b)

Figure 2. Stability region in the $\beta - \gamma$ plane. (a) Analysis, (b) Simulations

low values of k_i. It is important to note that until this point we only consider stability region of the linear part of system (31). The stability analysis of the entire system can be carried out using Lyapunov stability theory. We start by considering the Lyapunov function candidate

$$V[n] = e[n]^{'} P e[n] \ , \qquad P > 0$$

where P is a positive definite matrix and $e[n]'$ is the transpose vector of $e[n]$. System (31) is asymptotically stable if $V[n]$ is a decreasing sequence along any solution sequence $e[n]$; that is we need to show that $\Delta V[n] = V[n+1] - V[n] < 0$.

$$\Delta V[n] \quad = \quad e[n]^{'} \Big(\mathbb{A}^{'} P \mathbb{A} - P \Big) e[n] + 2 e[n]^{'} \mathbb{A}^{'} P f(e[n]) + f(e[n])^{'} P f(e[n]) \tag{40}$$

since $f(e[n])$ is a quadratic polynomial function, then it is a Lipschitz function, that is there exists k_f and R_f such that in the neighborhood of the origin we have:

$$|| \ f(e[n]) \ || \leq k_f \ || \ e[n] \ || \ , \qquad \forall \ || \ e[n] \ || \leq R_f \tag{41}$$

In fact, we can easily show by taking norm of $f(e[n])$ that

$$|| \ f(e[n]) \ || \leq 2\overline{k_v} \delta_m \mid e_1[n] \mid . \ || \ e[n] \ || \ , \qquad \delta_m = \max\{\delta_L, \delta_C\} \tag{42}$$

It is worth to note that $k_f = 2\overline{k_v}\delta_m \mid e_1[n] \mid$ explicitly depends on $\overline{k_v}$ and $e_1[n]$. Now, since $\mathbb{A}$ will be made stable by the choice of the design parameters then $\mathbb{A}^{'} P \mathbb{A} - P = -Q \ , \qquad Q > 0$ and therefore:

$$\Delta V[n] \leq -\Big(\lambda_{\min}(Q) - k_f (2 \ || \ \mathbb{A} \ || + k_f) \lambda_{\max}(P) \Big) \ || \ e[n] \ ||^2 \tag{43}$$

the proof of asymptotic stability is completed if we can find positive definite matrices P and Q such that the following relation is satisfied:

$$0 < \Big(\lambda_{\min}(Q) - k_f (2 \ || \ \mathbb{A} \ || + k_f) \lambda_{\max}(P) \Big) \tag{44}$$

As a matter of fact, we can say that for any given pair of matrices P and Q, and for $\overline{k_v} = k_v^s$, we can define a stability domain using $\mid e_1[n] \mid$ such that the obtained k_f makes condition (44) true. Although, theoretically the stability domain may vary with the choice of P and Q, simulations confirmed that we can achieve stability over the whole practical state space that is the normalized state variables are within the unit interval.

In Fig.3-b,c,d, we present two dimensional bifurcation diagrams that confirm the stability region shown in brown and it is in well concordance with the shaded area obtained analytically. The white dashed line in the brown area delineates the optimal (k_i, δ) pairs (leading to fast response) obtained numerically.

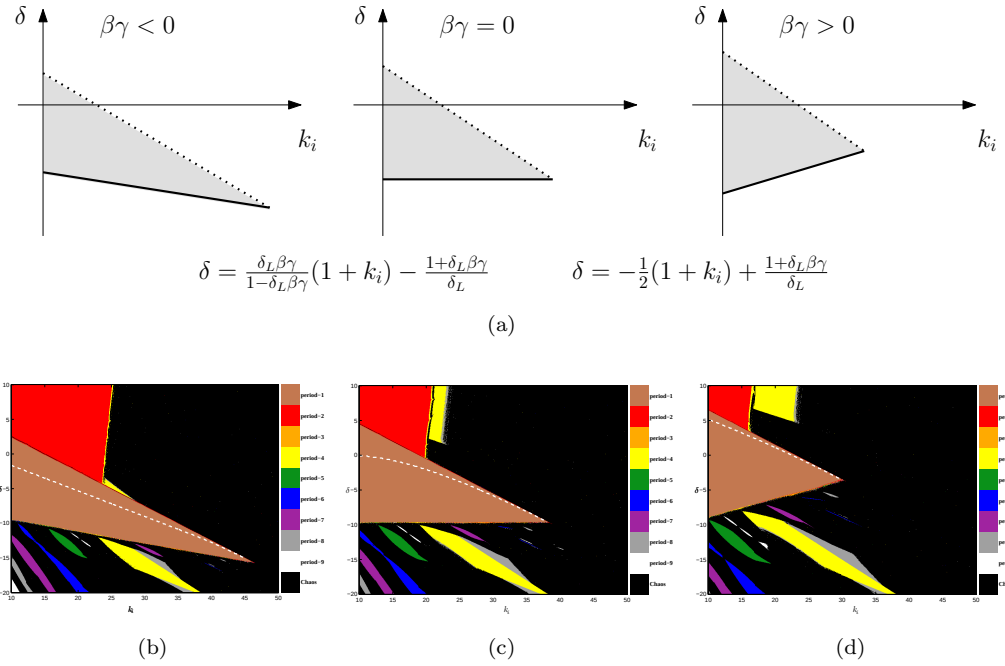

Figure 3. Two dimensional bifurcation diagram showing the behavior of the two-cell converter under the action of a dynamic TDFC for different values of the product $\beta\gamma$. Optimal pairs are represented with the white dashed line. Parameter values are: $\gamma = 1$, $k_v = k_{v,opt} = 8.33$, $k_{x,d} = 1$. (a) three cases from theoretical analysis. (b) $\beta = -2$, (c) $\beta = 0$ and (d) $\beta = 2$ from numerical simulations.

The effect of including the dynamic TDFC controller is tested using the simplified model and its performances are compared with those of a PI controller. The value of the proportional gain is the same for both controllers and the time constant of the PI controller is $\tau_{i,opt} = 1-\delta_L = 0.9$ which is an optimum choice in terms of the velocity of the system response in the linear (unsaturated) region. Figure 4 shows the evolution of the current and voltage of the system under the action of a dynamic TDFC controller with different parameters. The results are

compared with an optimized design of a PI controller (Fig. 5). We clearly observe that the generalized dynamic TDFC controller outperforms the PI controller and achieves the correct reference value in shorter settling time.

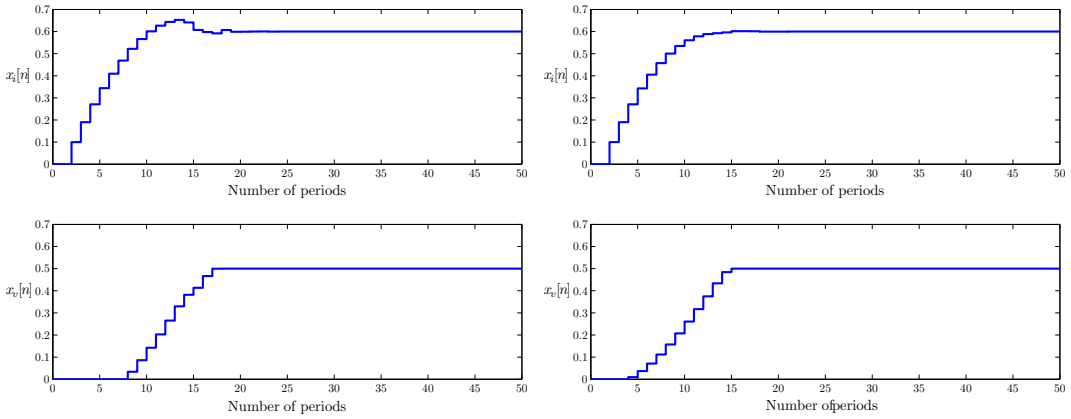

(a) (b)

Figure 4. Time evolution of the state variables from the simplified model under the action of a dynamic TDFC controller. (a) $k_i = 9$, (b) $k_i = 30$. Other parameters are $\beta = -2$, $\gamma = 1$, $k_v = k_{v,opt} = 8.33$, $k_{x,u} = 1$, $\delta = -7.245$.

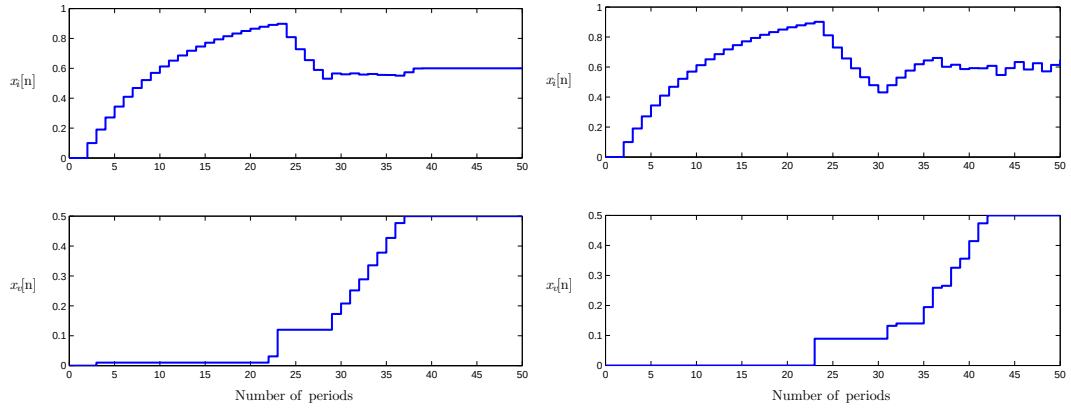

(a) (b)

Figure 5. Time evolution of the state variables from the simplified model under the action of a PI controller. (a) $k_i = 9$, (b) $k_i = 30$. Time constant τ_i is optimized ($\tau_i = \tau_{i,opt} = 1 - \delta_L = 0.9$) to get the faster response in the vicinity of the fixed point $\tau_i = 0.9$.

5. Controller validation using the switched circuit-based model

In order to illustrate the validation of the resulted obtained from the mathematical model, numerical simulation results from a circuit-based switched model were carried out. The parameter values used for the power stage circuit are as follows: $R = 25\ \Omega$, $L = 10$ mH, $C = 16\ \mu$F, $V_{in} = 900$ V, $f_s = 25$ kHz, $I_{ref} = 21.6$ A. These parameter values give rise to the same normalized parameters used in the previous section.

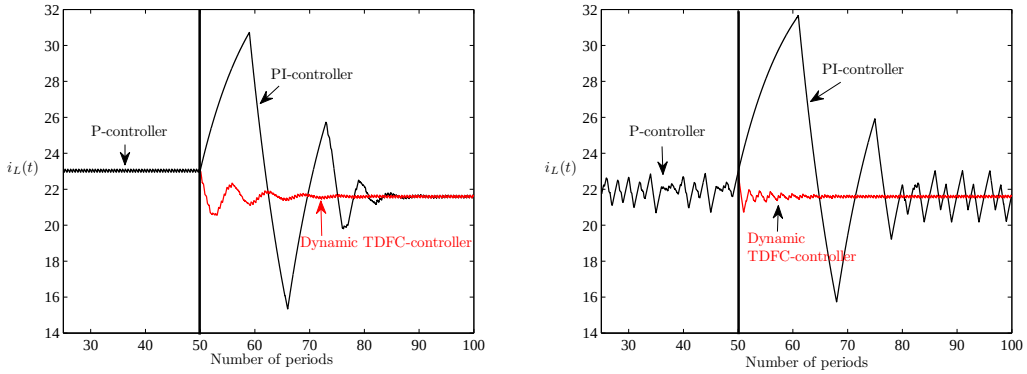

Figure 6. Validation of the results using the switched circuit-based model for two values of k_i (a) $k_i = 9$, (b) $k_i = 29$. Other parameters are $R = 25\ \Omega$, $L = 10$ mH, $C = 16\ \mu$F, $V_{in} = 900$ V, $f_s = 25$ kHz and $I_{ref} = 21.6$ A.

The results are shown in Fig. 6. In this figure we, during the first 50 period a simple proportional (P) controller is used. The control action is switched to a PI controller and to a dynamic TDFC controller at the moment $t = 50T$ for two values of the current gain k_i. As it can observed, with the dynamic TDFC controller, the system presents better performances in both cases. Furthermore, in the case of dynamic TDFC instabilities in the form of chaotic and subharmonic oscillations are avoided for higher values of the current gain k_i unlike the case of the PI controller for which these instabilities exist for the same value of k_i. Once the dynamic TDFC controller is added in the current feedback loop, the system is stabilized in its desired periodic regime with excellent static and dynamic performances. Furthermore, the comparison of the results shows that the simplified discrete time model and therefore the theoretical expressions for stability analysis, derived from this model are in good agreement with the simulation based on the exact switching model.

Conclusions

In this work, a new method for controlling and stabilizing a two-cell DC-DC buck converter by using a dynamic digital time delayed feedback was suggested. The proposed method has the same control effect as that of the PI control method in terms of steady state error. However, it has better performances such as shorter settling time and wider stability domain. The controller proposed herein, outperforms the traditional PI controller in terms of velocity of its response by appropriately choosing the feedback gain in terms of system parameters. In practice this can be achieved by adopting an adaptive control scheme in which the feedback gains can be updated cycle by cycle in terms of the system state variables. The proposed controller can be implemented easily and can be applied to other switched power converters. Further research will focus on the implementation of this control.

Acknowledgment

The authors would like to thank the anonymous reviewers for their comments and suggestion to improve an original version of this manuscript. This work was prepared within a Tunisian-Spanish cooperation framework, under grant A/6828/06 and A/021698/08 and by the Spanish Ministerio de Educación e Innovación under grant DPI2010-16481.

REFERENCES

1. Meynard, T. A., Fadel, M., Aouda, N., Modeling of multilevel converters. *IEEE Trans. Ind. Electronics* 44 (3), 356–364, 1997.
2. Tolbert, L. M., Peng, F. Z., Multilevel converters as a utility interface for renewable energy systems. in: IEEE *Power Engineering Society Summer Meeting*, pp. 1271–1274, 2000.
3. Huang-Jen Chiu, Chun-Jen Yao, Yu-Kang Lo, "A DC/DC converter topology for renewable energy systems", *International Journal of Circuit Theory and Applications*, vol. 37, no. 3, 2009, pp. 485-495
4. Thierry A. Meynard, Henri Foch, Philippe Thom, "Multicell Converters: Basic Concepts and Industry Applications", *IEEE Trans. on Ind Electronics,*, vol. 49, no. 5, pp. 955-964, 2002.
5. Meynard, T.A., Foch, H., Thomas, P., Courault, J., Jakob, R., Nahrstaedt, M., "Multicell converters: basic concepts and industry applications," *IEEE Transactions on Industrial Electronics,* vol. 49 no. 5 pp. 955-964, 2002.
6. Yousefzadeh V., Alarcón E., Maksimovic D, Three-Level Buck Converter for Envelope Tracking in RF Power Amplifiers, APEC'05- *IEEE Applied Power Electronics Conference*, Austin, Texas, 2005.
7. Middelbrook R. D and Cuk S, "A General Unified Approach to Modelling Switching Converters Power Stage", vol 1 and 2, Teslaco, Pasadena, C.A, pp. 73-89, 1983.
8. Béthoux O., Barbot J.-P. and Hilairet M., "Multicell actuator based on a sliding mode control", *Eur. Phys. J. Appl. Phys.* vol. 43, pp. 217-223, 2008.
9. Mohammad Hejri, Hossein Mokhtari, "Global hybrid modeling and control of a buck converter: A novel concept", *International Journal of Circuit Theory and Applications*, vol. , no. 9, pp. 968-986, 2009.

10. Alvarez-Ramirez, G. Espinosa-Pérez, D. Noriega-Pineda "Current-mode control of DC-DC power converters: a backstepping approach", *International Journal of Robust and Nonlinear Control*, vol. 13, no. 5, pp. 421-442, 2003.
11. Femia N., Fortunato M., Petrone G., Spagnuolo G., Vitelli M., "Dynamic model of one-cycle control for converters operating in continuous and discontinuous conduction modes" *International Journal of Circuit Theory and Applications*, vol. 37, no. 5, pp. 661-684, 2009.
12. Tse, C.K., 1994, Chaos from a Buck Switching Regulator Operating in Discontinuous Mode, *Int. J. Circuit Th. Appls.* (4), 263-278, 1994.
13. Nagy, I., Nonlinear dynamics in power electronics. in: *Proc. Electrical Drives and Power Electronics Conf.* pp. 1–15, 2000.
14. Robert, B., Robert, C., Border collision bifurcations in a one-dimensional piecewise smooth map for a pwm current-programmed H-bridge inverter. *International Journal of Control*, 75, 1356–1367, 2002.
15. Huang Y., Iu H. C. , Tse C. K, "Boundaries between fast- and slow-scale bifurcations in parallel-connected buck converters", *International Journal of Circuit Theory and Applications*, vol. 36, no. 5, 681-695, 2008.
16. Giaouris D., Maity S., Banerjee S., Pickert V., Zahawi B., "Application of Filippov method for the analysis of subharmonic instability in dc-dc converters", *International Journal of Circuit Theory and Applications*, 2008, DOI: 10.1002/cta.505.
17. El Aroudi A, Angulo F., Robert B. G. M, Olivar G., and Feki M., Stabilizing a Two-Cell DC-DC Buck Converter by Fixed Point Induced Control. *International Journal of Bifurcation & Chaos*, vol. 19, no. 6, pp. 2043-2057, 2009.
18. William C. Y. Chan, C. K. Tse, "Bifurcations in current-programmed DC/DC buck switching regulators-conjecturing a universal bifurcation path" *International Journal of Circuit Theory and Applications*, vol. 26, no. 2, pp. 127-145, 1998.
19. Robert, B. and El Aroudi, A., 2006, Discrete Time Model of a Multi-Cell DC/DC Converter, Non Linear Approach, *Mathematics and Computers in Simulation* 71(4-6), pp-310-319, 2006.
20. El Aroudi, A., Robert, B., Cid-Pastor, A., Martínez-Salamero, L., 2008, Modelling and Design Rules of a Two-Cell Buck Converter Under a Digital PWM Controller. *IEEE Transactions on Power Electronics*, vol. 23, no. 2, pp. 859-870, 2008.
21. Robert B., Feki M., Iu H.H.C., "Control of PWM Inverter Using a Proportional Plus Extended Time-Delayed Feedback Controller, *International Journal of Bifurcation and Chaos*, Vol. 16, No. 1, 113-128, 2006.
22. Batlle, C., Fossas E., and Olivar, G., Stabilization of periodic orbits of the buck converter by time-delayed feedback, *International Journal of Circuit Theory and Applications*, vol. 27, no. 5, pp. 617-631, 1997.
23. Tian Y. P, and Yu X., "Stabilizing unstable periodic orbits of chaotic systems via an optimal principle", *Journal of the Franklin Institute* vol. 337, pp. 771-779, 2000
24. Yamamoto S., Hino T., and Ushio T., "Dynamic Delayed Feedback Controllers for Chaotic Discrete-Time Systems", *IEEE Transactions on Circuits and Systems I*, vol. 48, no. 6, pp. 785-789, 2001.
25. Bai, X.-M., Li, H.-M., Yang, X.-S., 2006. Some results on cascade discrete-time systems. *Discrete Dynamics in Nature and Society* (DOI 10.1155/DDNS/2006/14631), pp. 1–8, 2006.

